Recent JET Experiments on Alfvén Eigenmodes with Intermediate Toroidal Mode Numbers: Measurements and Modelling

D.Testa[1], N.Mellet[1,2], T.Panis[1], S.E.Sharapov[3], D.Spong[4], P.Blanchard[1,5], H.Carfantan[6], A.Fasoli[1], A.Goodyear[3], and JET-EFDA contributors[*]
JET-EFDA, Culham Science Centre, Abingdon, OX14 3DB, UK

1) Ecole Polytechnique Fédérale de Lausanne (EPFL), Centre de Recherches en Physique des Plasmas (CRPP), Association EURATOM – Confédération Suisse, Lausanne, CH
2) Association Euratom – CEA, Cadarache, Saint-Paul-lez-Durance, France
3) Culham Centre for Fusion Energy, Culham Science Centre, Abingdon, UK
4) Oak Ridge National Laboratory, Fusion Energy Theory Group, Oak Ridge, USA
5) EFDA-CSU, Culham Science Centre, Abingdon, UK
6) Laboratoire d'Astrophysique de Toulouse – Tarbes, Université de Toulouse – CNRS, FR

e-mail contact of corresponding author: duccio.testa@epfl.ch

Abstract. This paper reports the results of recent experiments performed on the JET tokamak on Alfvén Eigenmodes (AEs) with toroidal mode number (n) in the range n=3-15. The stability properties and the use of these medium-n AEs for diagnostic purposes is investigated experimentally using a new set of compact in-vessel antennas, providing a direct and real-time measurement of the frequency, damping rate and amplitude for each individual toroidal mode number. First, we report on the development of a new algorithm for mode detection and discrimination using the Sparse Signal Representation theory. The speed and accuracy of this algorithm has made it possible to use it in our plant control software, allowing real-time tracking of individual modes during the evolution of the plasma background on a 1ms time scale. Second, we report the first quantitative analysis of the measurements of the damping rate for stable n=3 and n=7 Toroidal AEs as function of the plasma elongation. The damping rate for these modes increases for increasing elongation, as previously found in JET for n=0-2 AEs. A theoretical analysis of these JET data has been performed with the LEMan, CASTOR and TAEFL codes. The LEMan and TAEFL results are in good agreement with the measurements for all magnetic configurations where there is only a minor up/down asymmetry in the plasma poloidal cross-section. The CASTOR results indicate that continuum damping is not the only mechanism affecting the stability of these medium-n AEs. The diagnostic potential of these modes has being confirmed during the recent gas change-over experiment, where independent measurements of the effective plasma isotope ratio A_{EFF} have been provided in addition to the more routinely employed spectroscopic and gas-balance ones. These data shows a slight difference in the measurement of A_{EFF} when using n<5 and n>7 modes, suggesting a radial dependence in the effective plasma isotope ratio.

1. Introduction and Background: the new JET Alfvén Eigenmodes diagnostic.

The stability of Alfvén Eigenmodes (AEs) and the effect of these modes on the energy and spatial distribution of fast ions, including fusion generated αs, are among the most important issues for the operation of burning plasma experiments such as ITER. Of particular interest are AEs with toroidal mode number (n) in the range n~3-20, as these are expected to interact most strongly with the αs. The stability of these medium-n AEs is investigated experimentally in JET using an active system (the so-called Alfvén Eigenmodes Active Diagnostic, AEAD) based on a set of eight compact in-vessel antennas and real-time detection and discrimination of the individual n-components in the measured magnetic ($|\omega\delta B_{MEAS}|$) spectrum [1-3]. The AEAD system can now provide in real-time a direct measurement of the damping rate (γ/ω) as function of the dynamical evolution of the background plasma parameters, separately for all the antenna-driven toroidal mode numbers. The AEAD system consists principally of:
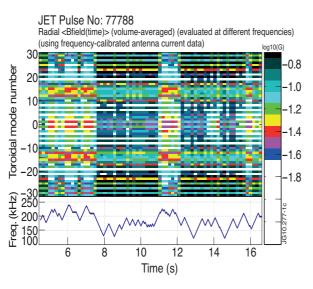1. the AE exciter, built upon a function generator and a high-power amplifier connected to a set of up to eight in-vessel antennas, whose aim is to send power into the plasma in order to

---

drive a very small magnetic perturbation, $\max(|\delta B_{DRIVEN}|)\sim 0.1G$ at the plasma edge, i.e. 10^5 times smaller than the typical value of the toroidal magnetic field in JET, $B_{TOR}\sim(1-3)T$;

2. a receiver, built upon synchronous detection units, which collects signals from various in-vessel detectors (magnetic pick-up coils, electron cyclotron emission, reflectometry); this receiver is also connected to the real-time AE Local Manager (AELM) to allow the detection and tracking of antenna-driven plasma resonances with different toroidal mode numbers.

The AE exciter uses a 5kW power amplifier capable of delivering up to a maximum antenna current and voltage $I_{ANT}\sim10A$-peak and $V_{ANT}\sim1kV$-peak, respectively, in the frequency range $10\rightarrow500kHz$ to each of the eight in-vessel antennas. The antennas are installed in two groups of four closely-spaced units at two toroidally opposite positions, at the same poloidal location. Any combination of these eight antennas can be chosen with a $\pm$ relative phasing to drive magnetic fluctuations with $|\delta B_{DRIVEN}|>10^{-3}G$ at the plasma edge. Hence, a very broad toroidal spectrum is excited for any antenna frequency, comprising many components, usually up to $|n|\sim30$, of which the higher-n ones are more strongly attenuated as function of the distance from the antennas. An example of the antenna-driven, volume-averaged, radial magnetic field $B_{RAD}(n,t)$ is shown in fig1 for the JET shot #77788 as function of the antenna frequency: note that up to two orders of magnitude difference in the driven $B_{RAD}(n,t)$ is seen between its different n-components up to $|n|\leq30$, which makes it an essential requirement to be able to discriminate in real-time the different n-components in the measured $|\omega\delta B_{MEAS}|$ spectrum.
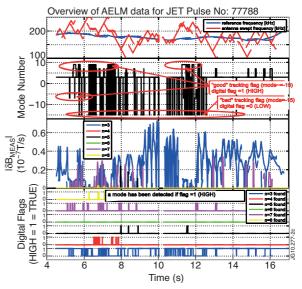

Figure1. The calculated antenna-driven, volume-averaged, radial magnetic field $B_{RAD}(n,t)$ for the JET shot #77788: note the large variation in B_{RAD} between the different n-components as the plasma background evolves and the antenna frequency is swept around the TAE frequency.

Figure2. Real-time discrimination between the different toroidal components in the frequency-degenerated AE spectrum driven by the new antennas for the JET shot #77788; the calculation is performed using a CPU-time of $<600\mu s$ within each 1ms AELM clock cycle.
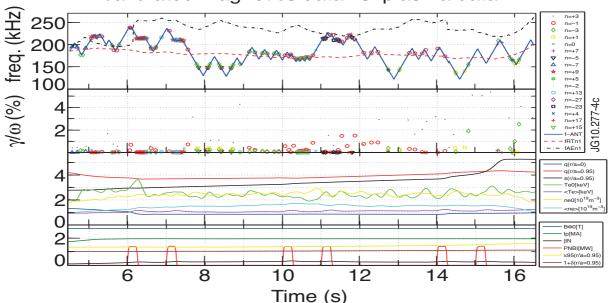
Given the close toroidal proximity between the four antennas in each of the two groups, a frequency-degenerated spectrum of plasma resonances is routinely obtained, i.e. one where the half-width at half-maximum of the modes (a quantity closely related to the damping rate) is comparable to their separation in frequency. This experimental observation has motivated the development of a novel method for mode detection and n-number discrimination using the Sparse Signal Representation theory and the SparSpec algorithm [4, 5], which has now been fully implemented in the AELM [6, 7]. The speed and accuracy of the SparSpec algorithm has made it possible to deploy it in our plant control software, allowing real-time tracking of the individual n-modes during the evolution of the plasma background on a sub-millisecond time

scale. An example of this real-time detection and discrimination of the concurrent n=3, n=5 and n=7 Toroidal AEs (TAEs) is shown in fig2 for the JET shot #77788, where the excitation system was configured to drive predominantly n-odd modes, with max($|\delta B_{DRIVEN}(n)|$) in the range $|n|\sim 3$-7, and producing a negligible drive for components with $|n|>10$.

2. Measurements of the Damping rate for Medium-n Alfvén Eigenmodes in JET.

The measurements of the damping rate for medium-n AEs are now being routinely obtained in different JET operating scenarios [3, 8]. An example of these data is shown in fig3 for the JET shots #77788 and #77790. In the latter, the AEAD system was configured to drive an odd-n spectrum peaked towards $|n|=7$-11, with a negligible drive for $|n|>15$ and $|n|<3$.
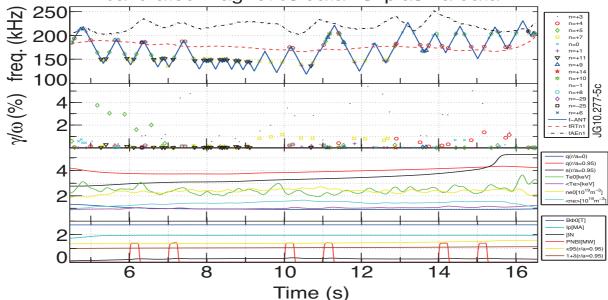

Figure3. Measurement of the damping rate for individual toroidal mode numbers for the JET shots #77788 (top) and #77790 (bottom) as function of the evolution of the main plasma parameters.

In JET, the edge plasma shape and magnetic shear have been found to be key ingredients for increasing the damping rate of stable, antenna-driven low-n (n=1, n=2) [9] and unstable, fast-ion driven, medium-n (n~3-10) TAEs [10]. This has motivated experimental studies on the Alcator C-mod tokamak where it was found that the damping rate of an n=6 TAE remains essentially invariant when the average edge triangularity (δ_{95}) is scanned in the range $0.3<\delta_{95}<0.7$ [11]. Conversely, the data obtained for the n=3 and n=7 TAEs during the two otherwise similar JET discharges presented in fig3 show an almost linear increase of the damping rate as a function of the edge elongation (κ_{95}). Hence, increasing κ_{95} has in JET the same effect on the damping rate of these medium-n TAEs as on the n=1 and the n=2 TAEs. This result further confirms that the same damping mechanisms acting upon global, low-n modes, play also an important role for the stability of core-localised medium-n TAEs, opening interesting perspectives for their real-time control in burning plasma experiments.

The two discharges shown in fig3 have been used for detailed comparisons with theory and models in the framework of the ITPA work-program [12]. Figure4 shows the measurements of the damping rate for n=3 and n=7 TAEs as function of the edge elongation in ohmic plasmas together with the results of simulations performed with the LEMan [13, 14], TAEFL [15, 16] and CASTOR [17] codes. Both the LEMan and the TAEFL codes model the actual plasma shape using a magnetic configuration which is up/down symmetric, but non-circular.
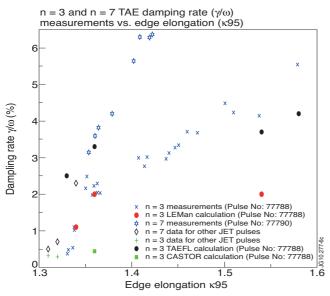

Figure4. Damping rate data for the n=3 and n=7 TAEs as function of κ_{95}, showing a linear dependence $\gamma/\omega=f(\kappa_{95})$, compared with the results of the LEMan, TAEFL and CASTOR simulations.

The LEMan results [8] show that, for the cases where the actual plasma poloidal cross section is sufficiently up/down symmetric, the mode frequency and damping rate are in good agreement with the measurements (mode frequencies within 10%, damping rates within ~50%), this exercise also demonstrating that a rather large number of poloidal harmonics needs to be used to reproduce quantitatively the measured γ/ω even for moderately low-n modes. Conversely, when the up/down asymmetry in the poloidal cross-section is not correctly retained in LEMan (i.e. for $\kappa_{95}>1.45$), there is a much larger discrepancy, up to a factor ~2, between the measured and the calculated damping rates.

The TAEFL code is a reduced MHD initial value code that uses gyrofluid closure techniques for the energetic ions to incorporate the Landau resonance effects that destabilize Alfvén modes. Since only unstable modes can be analyzed by TAEFL, the technique used was to start with an unstable Alfvén mode, vary the fast ion drive and extrapolate back to zero drive in order to determine an effective damping rate. Fast ion profiles/parameters are chosen that lead to a mode very close to the frequency excited by the antenna. This model incorporates ion/electron Landau damping, continuum damping and radiative damping (due to finite ion Larmor radius) effects. It uses Fourier spectral representations in the poloidal and toroidal directions and finite differences in the direction normal to the flux surfaces. The TAEFL simulations of JET plasmas used 300-400 radial points and 26 Fourier modes (m=0→25). The TAEFL results are in very good agreement with the measurements for relative high values of the elongation ($\kappa_{95}>1.45$), whereas the discrepancy at lower values of κ_{95} is somewhat larger.

Figure5 shows the results of the simulations performed with the CASTOR code for the shear Alfvén continuum and radial Eigenfunction (rV_r) for the n=3 TAE in the JET shot #77788 at t=10.1sec. These calculations used 11 poloidal harmonics (m=3→13), the resistivity was set to $\eta=1\times10^{-7}$, and the radial extent was set to s=sqrt(ψ_N)=0→0.95, where ψ_N is the normalized poloidal flux. The CASTOR code predicts an n=3 mode at 184kHz (in good agreement with the measurement: f_{MEAS}=179kHz) with a damping rate γ/ω_{CASTOR}=0.44%, compared to γ/ω_{MEAS}~2.0%. The discrepancy with the measured damping rate can be due to small uncertainties in the q- and/or density profiles, and to the absence of kinetic effects. For instance, slightly different values of q- or density at ψ_N~0.55 can make the mode intersect the continuum and increase γ/ω_{CASTOR} by a factor of 2, and kinetic effects such as radiative and Landau damping have been shown to play an important role with other codes such as LEMan and LIGKA [18]. Hence continuum damping, which is the only mechanism included in these CASTOR simulations, can only account for a fraction of the measured damping rate, which clearly suggests that other mechanisms make important contributions to the total damping.
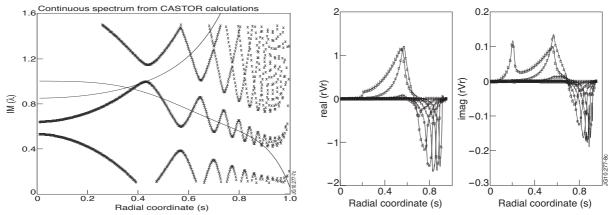

Figure5a. The shear Alfvén continuum (left) and the radial Eigenfunction rV_r (right) calculated by the CASTOR code for the n=3 TAE in the JET shot #77788 at t=10.100sec.
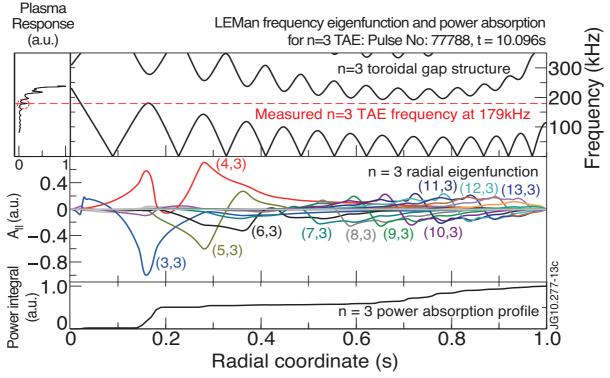

Figure6. The antenna loading, the continuum, the radial Eigenfunction and the power absorption as calculated by the LEMan code for the n=3 TAE in the JET shot #77788 at t=10.096sec.

Again for the n=3 Eigenmode in #77788, fig6 shows the antenna loading, the continuum, the radial Eigenfunction and the power absorption calculated by the LEMan code at t=10.096sec, and fig7 shows the radial Eigenfunction and the 2D contour plot of the Eigenmode calculated by the TAEFL code at t=10.248sec, t=14.261sec and t=15.835sec.
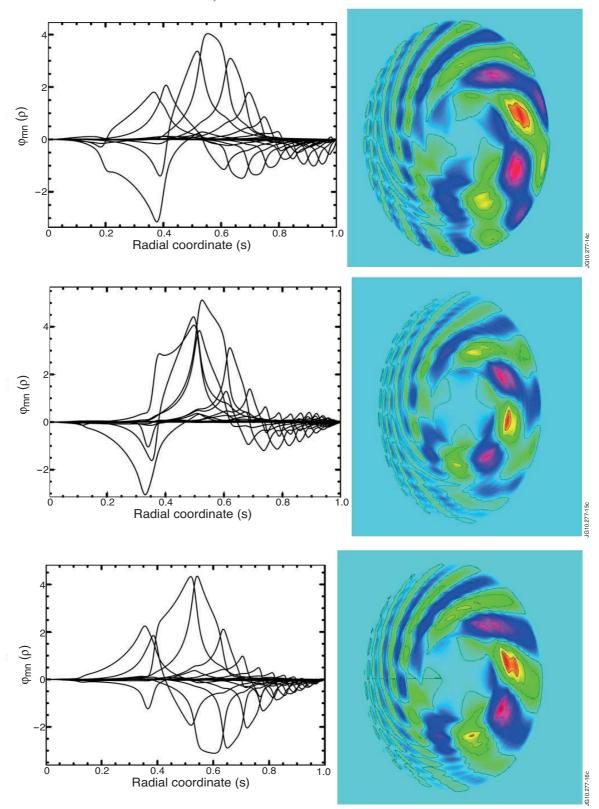

Figure7. The radial Eigenfunction (left) and the 2D contour plot (right) of the Eigenmode as calculated by the TAEFL code for the n=3 TAE in the JET shot #77788 at t=10.248sec (top frame), t=14.261sec (middle frame) and t=15.835sec (bottom frame).

It is important to note that, despite the differences between the codes, the radial Eigenfunction computed by CASTOR, TAEFL and LEMan are in sufficiently good agreement between each other, indicating a good understanding of the physics mechanisms contributing to determining the stability of these medium-n AEs, and of the effect that the differences between the various codes and models can have on the predictions for ITER [12].

3. Diagnostic Use of Medium-n Alfvén Eigenmodes in JET.

The diagnostic potential of medium-n AEs has being confirmed during the recent gas change-over experiments in JET, where the AEAD system has provided independent measurements, up to 10ms time-resolved, of the plasma isotope ratio A_{EFF} in addition to the more routinely employed (but slower) spectroscopic and gas-balance ones.
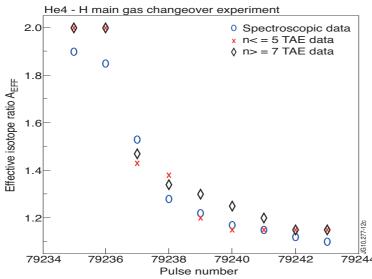

Figure8. Measurement of the plasma effective isotope ratio A_{EFF} during the gas change-over experiments in JET.

These measurements have been previously performed on JET using radially extended low-n TAEs [19], and have been proven to agree very well with the slower data obtained using the low-energy Neutral Particle Analyser and the Charge Exchange diagnostics [20]. The AE-derived measurement of A_{EFF} is obtained by comparing the value of the Alfvén frequency F_{ALFVEN} for modes with the same toroidal mode number in discharges with a similar (within error bars) magnetic configuration, current profile and plasma shape.

The AE diagnostic can in principle provide a spatial resolution for $A_{EFF}(r)$ if different n's are measured during similar discharges. The value of A_{EFF} is obtained using the definition (where Z_{EFF} is the plasma effective charge, $q_{TAE}=(2m+1)/2n$ and R_{TAE} are the safety factor and radial position of the gap associated with the mode with poloidal and toroidal mode numbers m,n):

$$F_{ALFVEN} = \frac{V_{ALFVEN}}{4\pi q_{TAE} R_{TAE}} \propto \frac{1}{\sqrt{A_{EFF}}} \ , \quad A_{EFF} = \frac{\sum_i n_i \left(m_i \Big/ m_p \right)}{\sum_i n_i} \approx \frac{1}{n_e / Z_{EFF}} \sum_i n_i A_i \ .$$

The data presented in fig8 indicate a slight, but very clear, difference in $A_{EFF}(n)$ for TAEs with n≤5 (more global) and n≥7 (more core-localised), hence suggesting a radial dependence in $A_{EFF}(r)$ which could have not been easily picked-up by other diagnostic systems.

4. Conclusions.

A new algorithm, based on the Sparse Representation of signals, has been developed and fully implemented to discriminate in real-time the different toroidal components in the plasma response to the multi-components, frequency-degenerate, magnetic field spectrum driven by the new AE antennas in JET. The quantitative analysis of the first damping rate measurements obtained in JET for n=3 and n=7 TAEs has confirmed the experimental scaling of an increase

in γ/ω as the edge elongation (hence the edge magnetic shear) is increased. This scaling agrees very well with previous JET data for low-n TAEs, and with theoretical estimates based on mode conversion of TAEs to Kinetic Alfvén Waves. These new JET experimental results further confirm the possibility of using the edge shape parameters as a real-time actuator for the control of the AE stability in burning plasma experiments. Detailed simulations performed with the LEMan, TAEFL and CASTOR codes have demonstrated the need to include in the calculations the up/down asymmetry in the plasma poloidal cross-section, a large number of poloidal harmonics, and that continuum damping is not the only mechanism accounting for the measured damping rate for these modes. Finally, the diagnostic potential of medium-n AEs has also been demonstrated with the measurement of the plasma effective isotope ratio, opening further possible perspective for the use of an AE-based diagnostic system in ITER.

References.
1. Fasoli, A., et al., Phys. Rev. Lett. **75**(4) (1995), 645.
2. Testa, D., et al., "The new Alfvén Wave Active Excitation System at JET", Proceedings 23rd SOFT Conference (2004); weblink: http://infoscience.epfl.ch/record/143354/files/.
3. Panis, T., Testa, D. et al., Nucl. Fusion **50** (2010), 084019.
4. Bourguignon, S., Carfantan, H., Böhm, T., Astronomy and Astrophysics **462** (2007), 379.
5. Klein, A., Carfantan, H., Testa, D. et al., Plasma Phys. Control. Fusion 50 (2008), 125005.
6. Testa, D., et al., "The JET Alfvén Eigenmode Local Manager for the real-time detection and tracking of a frequency-degenerate spectrum of MHD instabilities", submitted for publication to Fusion Engineering and Design, August 2010.
7. Testa, D., et al., "An algorithm for the real-time and unsupervised detection, decomposition and tracking of the individual components in a degenerate, multi-harmonics spectrum", submitted for publication to EuroPhysics Letters, June 2010.
8. Testa, D., et al., Nucl. Fusion **50** (2010), 084010.
9. Testa, D., and Fasoli, A., Nucl. Fusion **41** (2001), 809.
10. Testa, D., Fasoli, A., Borba, D., et al., Plasma Phys. Control. Fusion **46** (2004), S59.
11. Snipes, J.A., Basse, N., Boswell, C., et al., Phys. Plasmas **12** (2005), 056102.
12. Lauber. Ph., et al., paper THW/P7-08, IAEA-FEC 2010.
13. Popovich, P., Cooper W.A., and Villard, L., Comput. Phys. Comm. **175** (2006), 250.
14. Mellet, N., CRPP-EPFL PhD Thesis (weblink: http://library.epfl.ch/theses/?nr=4398).
15. Spong, D.A., Carreras, B.A., and Hedrick, C.L., Phys Fluids B-Plasma **4**, 3316 (1992).
16. Spong, D.A., Carreras, B.A., and Hedrick, C.L., Phys Plasmas **1**, 1503 (1994).
17. Kerner, W., Goedbloed, J.P., et al., Journal of Computational Physics **142** (1998), 271.
18. Lauber, Ph., Günter, S., et al., Journal Computational Physics **226** (2007), 447.
19. Fasoli, A., Testa, D., et al., Plasma Phys. Control. Fusion **44** (2002), 159.
20. Bettella, D., Testa, D., et al., Plasma Phys. Control. Fusion **45** (2003), 1893.